Available online at www.sciencedirect.com
ScienceDirect
Journal of Bionic Engineering 11 (2014) 620–629

Wear Resistance and Non-Magnetic Layer Formation on 316L Implant Material with Plasma Nitriding

Ali Fatih Yetim[1], Mustafa Yazıcı[2]

1. *Department of Mechanical Engineering*, *Faculty of Engineering and Architecture*, *Erzurum Technical University*, *Erzurum* 25700, *Turkey*
2. *Department of Nanoscience and Nanoengineering*, *Ataturk University*, *Erzurum* 25240, *Turkey*

Abstract

In this study, the applicability of plasma nitriding treatment in the production of non-magnetic and corrosion resistant layer on 316L stainless steel implant material was investigated. 316L stainless steel substrates were plasma nitrided at temperatures of 350 ˚C, 375 ˚C, 400 ˚C, 425 ˚C and 450 ˚C for 2 h in a gas mixture of 50% N_2–50% H_2, respectively. It was determined that the treatment temperature is the most important factor on the properties of the corrosion resistant layer of 316L stainless steel. The results show that s-phase formed at the temperatures under 400 ˚C, and at the temperatures above 400 ˚C, instead of s-phase, CrN and γ'-Fe_4N phases were observed in the modified layer. The electrical resistivity and surface roughness of the modified layer increase with treatment temperature. Under 400 ˚C the corrosion resistance increased with the temperature, above 400 ˚C it decreased with the increase in treatment temperature. It was analyzed that the electrical resistivity and the soft (ideal) ferromagnetic properties of 316L stainless steel increased with treatment temperature during nitriding treatment. Also, plasma nitriding at low temperatures provided magnetic behavior close to the ideal untreated 316L stainless steel.

Keywords: 316L stainless steel, biomaterials, plasma nitriding, magnetic properties, wear, electrical resistivity

doi: 10.1016/S1672-6529(14)60073-1

1 Introduction

Austenitic stainless steels are widely used in many areas such as aerospace, military, automotive industry, chemical processing and biomedical engineering as an implant material because of their magnetization properties and corrosion resistance[1]. However, their friction coefficients, hardness and wear resistance are generally thought insufficient. The surface treatments have been applied to improve these inadequate properties[2]. Various surface modification methods such as the ion implantation, plasma assisted thermochemical treatment and thin film deposition such as Physical Vapor Deposition (PVD) and Chemical Vapor Deposition (CVD) are used to solve these problems[3–6]. Puchi-Cabrera *et al*.[7] deposited DLC films onto alloyed steel substrate, and the films exhibited high internal residual stresses, poor adhesion to the substrate and limited load-bearing capacity. Arslan *et al*.[8] studied that after plasma-nitriding treatment for austenitic stainless steel at different gas compositions of N_2–H_2 mixture at various temperatures for 1 h, s-phase was formed in the microstructure. With the formation of s-phase structure, corrosion resistance of samples was improved. Among these methods, nitriding treatment is more advantageous than the others due to its rapid coating capability, low cost and easy operation.

In many studies, it is indicated that the most important factor in nitriding treatment is temperature. Also, the temperature increment after 500 ˚C raises the nitrogen diffusion to the diffusion layer and precipitations of CrN and γ′-Fe_4N are formed. The increase of this dual phase structure may cause the deterioration of corrosion resistance[4]. The literature reports show that the expanded austenite (γ_N) or s-phase in the nitrided layer, which is known as a metastable phase, occurs at low temperatures. Also, these structures exhibit high hardness and wear resistance without losing their corrosion

Corresponding author: Ali Fatih Yetim
E-mail: fatih.yetim@erzurum.edu.tr

resistance[4,9–11]. There are many studies about this phase in the literature. Ichii *et al*.[12] described this metastable phase as s-phase. Singh *et al*.[13] concluded that the s-phase has a body-centered tetragonal lattice and designated this phase as the m-phase. Also, this phase shows very interesting magnetic properties. Gontijo *et al*.[14] indicated that the s-phase may be paramagnetic or ferromagnetic. It is believed that higher density of stacking fault and N content cause the lattice expansion that gives rise to ferromagnetism[15,16]. It is well known that the ceramic structure of materials is nonconductive. Omari and Sevostianov[17] demonstrated that the surface imperfections like gaps, dislocations and grain boundaries located within the structure reduce the conductivity of materials.

The biomaterials used as an implant material should have some properties like high wear resistance, hardness and corrosion resistance. In addition to these significant properties, implants should be produced with non-magnetic materials, because they can be subjected to the magnetic field in some applications such as Magnetic Resonance (MR) device. For that reason, non-magnetic materials are chosen and preferred such as austenitic stainless steel (316L, 304, *etc*.) in biomedical applications.

There are many studies on the wear, corrosion properties of the plasma nitrided 316L stainless steel, but enough studies on the magnetic and electrical properties of the formed s-phase of 316L stainless steel are not available. The aim of this study is to determine the optimum mechanical, tribological, magnetic and electrical properties of austenitic 316L stainless steel after plasma nitriding treatment. To achieve this aim, nitriding treatment was applied at temperatures of 350 ˚C, 375 ˚C, 400 ˚C, 425 ˚C and 450 ˚C for 2 h. The structure, surface morphology, microhardness, wear resistance, corrosion resistance, magnetic property, and electrical property of the modified layer were investigated.

2 Experimental details

316L stainless steel specimens from American Iron and Steel Institute (AISI) with 5 mm thickness were cut from cylindrical bars. The samples were grinded by 80–1200 mesh emery papers, and then polished with alumina powder with 0.5 μm and 0.3 μm grain sizes. After cleaning with alcohol, the specimens were placed into the plasma nitriding chamber and the chamber was evacuated to 3 Pa. Before the process, to clear the contaminants on the surface, the specimens were exposed to cleaning by hydrogen sputtering for 20 min under a voltage between 400 V – 500 V and a pressure of 5×10^2 Pa. The plasma nitriding was performed in the gas mixture of 50% H_2 and 50% N_2, at the treatment temperatures of 350 ˚C, 375 ˚C, 400 ˚C, 425 ˚C and 450 ˚C, for 2 h, respectively. Temperature was measured by a thermocouple inserted into the specimen holder cathode. For the structural characterization, XRD measurements were performed by using a Cu Kα (λ=1.5418 Å) source diffractometer with scanning angles from 30˚ to 65˚. The Match program was used for identification of phases. The cross-section of layers, the surface morphologies after plasma nitriding and surface morphologies after electrochemical and tribological examinations were investigated using a Scanning Electron Microscope (SEM) Jeol 6400. The dry wear tests were carried out on Turkyus PODTW&RWT pin-on-disk tester, using a 6 mm diameter Al_2O_3 ball as a pin. Also, wear tests with a sliding distance of 141 m were carried out at room temperature (≈18 ˚C) and a relative humidity of about 50%, a sliding speed of 0.078 ms^{-1}, normal load of 2 N and a wear track diameter of 10 mm. Five separate wear tests were performed and the average results was given.

Roughness measurements on the surface of the samples before and after the treatments were performed with the Mahr device. Hardness values with average five measurements for each group of specimens were measured by using Buehler Omnimet-MHT1600-4980T, with a Knoop indenter and at a load of 100 gr.

Electrochemical polarization experiments were performed using GAMRY Series G750™ Potentiostat/Galvanostat/ZRA device. One side of the specimen with an area of approximately 0.38 cm^2 was exposed to the solution. The polarization measurements were carried out in a corrosion cell containing Simulated Body Fluid (SBF) solution of 500 ml at 37 ˚C, and 7.4 pH. Content of the SBF solution suggested by Kokubo and Takadama was given in Table 1[18]. A stabilization period of 7200 s was employed before starting the measurement. The electrode potential was raised from −0.5 V to 1 V compared to OCP with the scanning rate of 1 $mV \cdot s^{-1}$, and the current that flowed through the diffusion layer-substrate system was recorded. For polarization measurements a three-electrode cell was used employing Ag/AgCl electrode as the reference electrode, graphite

Table 1 SBF content used in wear tests[18]

Ion	Na^+	K^+	Mg^{2+}	Ca^{2+}	Cl^-	HCO_3^-	HPO_4^{2-}	SO_4^{2-}	pH
Ion concentration in SBF (mM)	142.0	5.0	1.5	2.5	147.8	4.2	1.0	0.5	7.4

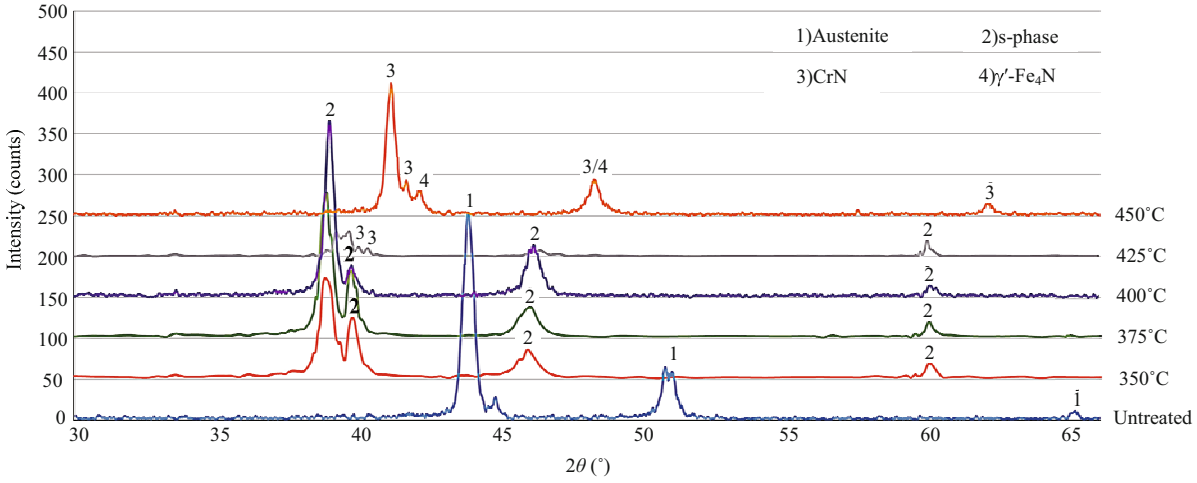

Fig. 1 XRD results of untreated and plasma nitrided samples.

bar as the counter electrode and working electrode, respectively.

The magnetic properties of 316L stainless steel specimens were measured with a Vibrating Sample Magnetometer (VSM) Physical Property Measurement System (PPMS) Quantum Design Model 6000 under various magnetic fields.

The electrical properties of 316L stainless steel specimens were measured both before and after treatment with PPMS Model 6000 using four point method.

3 Results and discussion

3.1 XRD analysis

XRD graphs of untreated and plasma nitrided samples are given in Fig. 1. XRD analysis shows that the microstructure of the untreated 316L stainless steel completely consists of austenite phase with a face centered cubic (fcc) structure. After the plasma nitriding, a modified layer was formed on the substrate. This layer includes of s-phase, CrN and γ'-Fe_4N phases depending on the nitriding temperature. In Fig. 1, it was observed that the peaks of s-phase formed at the temperatures lower than 400 ˚C. The γ'-Fe_4N and CrN phases occurred at the temperatures higher than 400 ˚C because the affinity of Cr and Fe atoms to nitrogen atoms increased and they tend to nitride compounds. Also, it can be said that the s-phase peaks, which formed by nitriding at the lower temperatures, are the shifting form of austenite peaks at lower reflected angles. When the temperature reached to 425 ˚C, the CrN starts to occur because the activation of nitrogen atoms increases. The s-phase is defined as expanded austenite lattice because of the effect of nitrogen atoms[19,20]. The formation of s-phase mainly depends on the treatment temperature. Nitrogen atoms begin to separate from austenite lattice with the increase in treatment temperature and these nitrogen atoms combine with chromium atoms that lead to the creation of nuclei CrN. The increase in treatment temperature led to a decrease in the amount of s-phase peaks and an increase in intensity of CrN. Besides, it was seen that the s-phases transformed to metastable γ′-Fe_4N phases with the increase in treatment temperature[21]. Stainless steels contain sufficient chromium to form a passive film of chromium oxide, which prevents further surface corrosion and blocks corrosion from spreading into the internal structure of the metal. The large amount of CrN compounds decreases the free chromium atoms in the stainless steel and this causes the loss of corrosion resistance of 316L austenitic stainless steel.

3.2 Microstructure and morphology

Fig. 2 shows some typical micrographs of the cross-sections of nitrided samples. A clear line that is seen as a homogeneous layer separated from the bulk material on the surface of all nitrided samples[19,21]. The thickness of the modified layer increases with the treatment temperature[19]. The mean thicknesses of these layers are given in Table 2. The thickness of modified layer was measured between 3 μm–17 μm. The minimum thickness was obtained from the samples nitrided at 350 ˚C for 2 h. The surface roughness values increased with the treatment temperature. The modified layers showed different characteristics dependent on the treatment temperature. s-phase was seen in white color in the modified layer. Therefore, it was thought that the amount of s-phase was more than those of CrN and γ'-Fe_4N phases, under 400 ˚C. Previous studies pointed out that the s-phase appeared light-colored due to its resistance to etchants[22]. As the treatment temperature increased, CrN and γ'-Fe_4N nitrides formed and the structure of the stainless steel converted from a metastable form to the stable form. This dual nitride form appeared as dark spots. When the treatment temperature approached to 450 ˚C, the amount of the nitrides (dark areas) increased and covered the whole layer (Fig. 2 d, e).

3.3 Microhardness

The microhardness values obtained from the cross-sections of the treated sample surfaces are given in Table 2. While the microhardness values of the untreated samples were measured as 270 $HV_{0.01}$–300 $HV_{0.01}$, those of the treated samples increased by almost four times after plasma nitriding. Results show that while the values of surface hardness decreased to substrate hardness under the modified layer, but the hardness values didn't change in modified layer line in nitrided samples. The lowest hardness value was measured on the samples nitrided at temperature 350 ˚C, while the highest hardness value was measured on the samples nitrided at temperature 450 ˚C. The hardness of modified layer depends on the substrate hardness, chemical composition and thickness of the modified layer. A harder substrate and a thicker modified layer can resist further plastic deformations. Thus, surface hardness increases. s-phase has high hardness due to lattice distortion caused by interstitial nitrogen atoms, therefore it depends on the concentration of nitrogen atoms[23]. The increasing temperature caused higher hardness values obtained with the increasing nitrogen intensity within the structure. At the temperature higher than 400 ˚C, s-phase decomposes and CrN+γ'-Fe_4N phases start to form. The nitrided layers containing CrN+γ'-Fe_4N dual phases

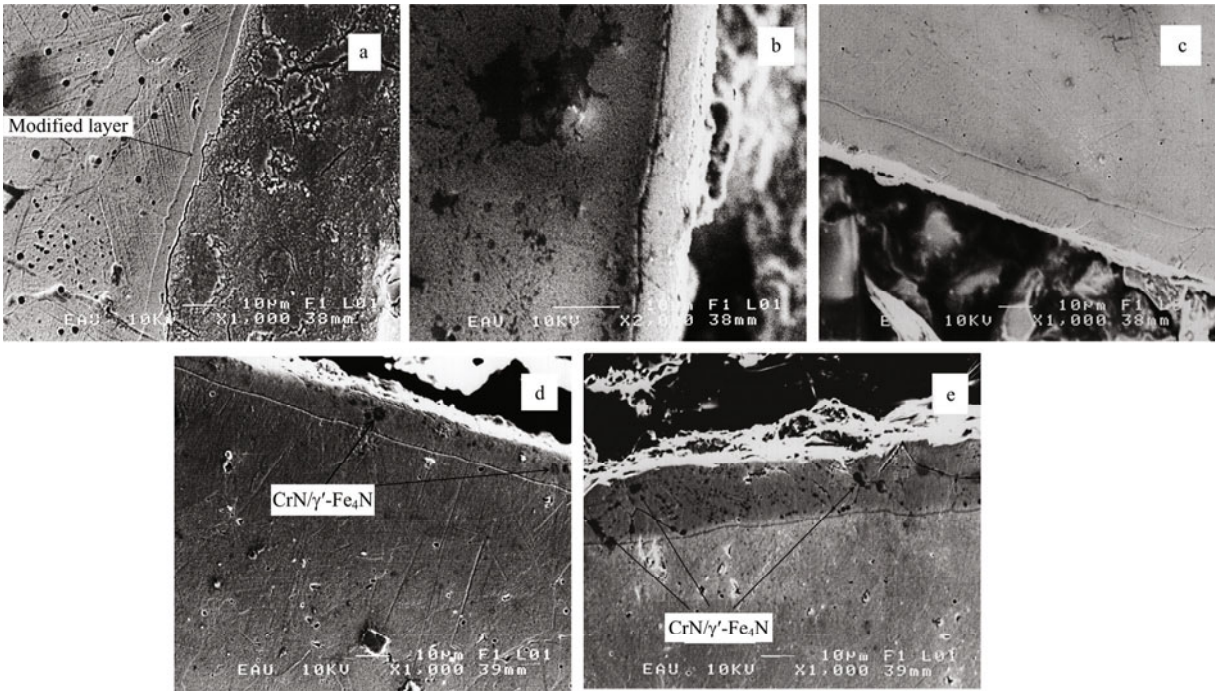

Fig. 2 Cross-section SEM micrographs of the nitrided samples. (a) 350 ˚C; (b) 375 ˚C; (c) 400 ˚C; (d) 425 ˚C and (e) 450 ˚C for 2 h.

Table 2 Changes in modified layer thickness, surface roughness and surface hardness of nitrided 316L for different treatment parameters

	Temperature (˚C)	Time (h)	Gas mixture	Modified layer thickness (μm)	Surface roughness (R_a)	Hardness ($HV_{0.01}$)
1	350	2	50%N_2 +50%H_2	3–4	0.07	450–480
2	375	2	50%N_2 +50%H_2	5–6	0.09	540–570
3	400	2	50%N_2 +50%H_2	8–10	0.11	650–680
4	425	2	50%N_2+50%H_2	10–12	0.22	950–1000
5	450	2	50%N_2 +50%H_2	15–17	0.34	1100–1150
Untreated 316L stainless steel	–	–	–	–	0.06	270–300

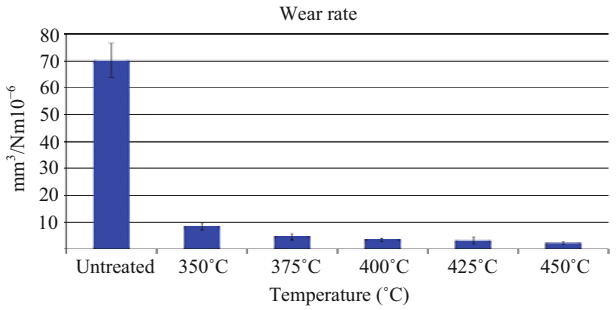

Fig. 3 Wear rate results of untreated and plasma nitrided samples.

were harder than the modified layer containing purely s-phase. Therefore, higher hardness values were measured when nitriding was performed at the temperatures higher than 400 ˚C because larger modified layer thickness and nitride phase structures were obtained at these treatment conditions.

3.4 Wear examination

The wear test results of the plasma nitrided and the untreated 316L stainless steel are shown in Fig. 3. The wear resistance of 316L stainless steel increased after the plasma nitriding. The wear rates of the nitrided samples for all nitriding parameters were lower than that of the untreated samples. Also, the wear rates of nitrided samples decreased with the increase in nitriding temperature. It was observed that wear resistance increased with nitriding temperature. At the higher temperatures, CrN+γ'-Fe_4N dual phase structure began to occur and wear resistance was improved because this dual phase structure had higher hardness than s-phase. Moreover, at higher temperatures, thicker modified layer, formed on the sample surface, was more capable to resist plastic deformation. Thus, the lowest wear rate was obtained from the samples nitrided at 450 ˚C for 2 h (Fig. 3). The wear tracks of the plasma nitrided and untreated 316L are shown in Fig. 4. For untreated 316L

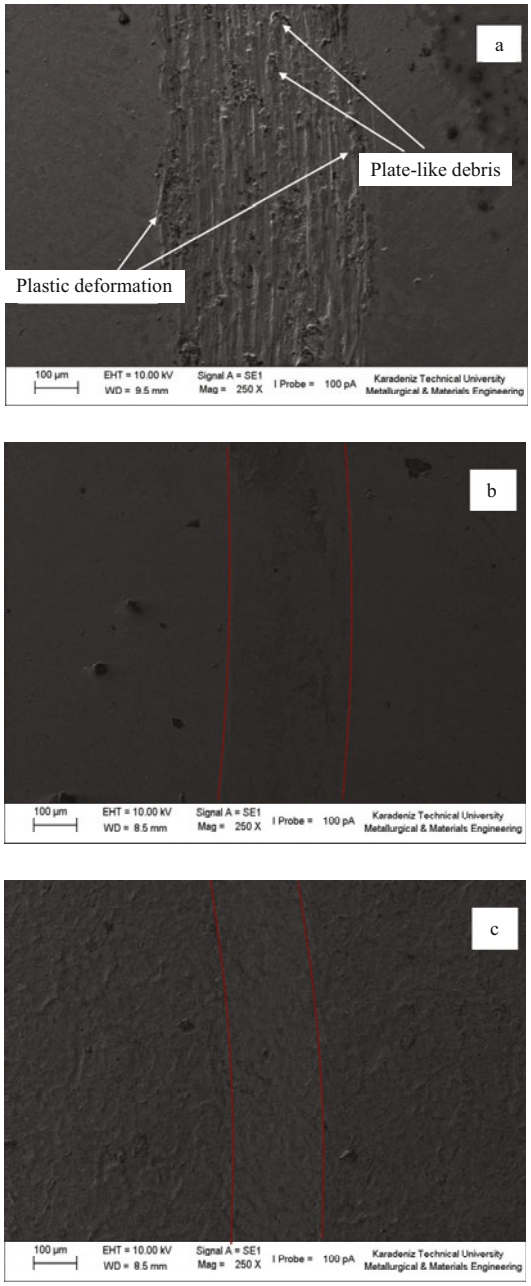

Fig. 4 SEM micrographs of wear tracks. (a) Untreated; (b) the sample plasma nitrided at 350 ˚C; (c) the sample plasma nitrided at 450 ˚C.

(Fig. 4a), it is seen that the wear modes were adhesive, abrasive and plastic deformation types. The crushed particles on the wear tracks indicated that untreated samples showed adhesive wear[24]. These particles were formed during the sliding between pin and surface. Also, the accommodation of wear debris on the sides of wear tracks implied excessive plastic deformation during sliding of the untreated 316L. On the other hand, plasma nitrided samples showed smooth and shallow wear scars because the hard modified surface caused a lower contact area between surface and pin. Some microabrasion grooves observed on the wear track of nitrided sample were due to hard particles broken from compound layer[4,25].

Friction test results of 316L stainless steel are illustrated in Fig. 5. While the average friction coefficient of the untreated specimens is 0.6, the friction coefficient changes between 0.65 and 0.85 after the nitriding. A run-in period behavior was seen for untreated samples. It was observed that friction coefficient suddenly increased due to Hertzian contact and reached a maximum value and then it decreased at the early stages of sliding. After 500 s, friction coefficient slowly increased again and stabilized as about 0.6. In the case of nitrided samples, it was assumed that surface roughness increased the friction coefficient values. So, higher friction coefficient values were obtained from the samples nitrided at higher temperatures.

3.5 Corrosion properties

The current densities versus potential graphs of the untreated and treated 316L stainless steel samples are shown in Fig. 6. The pitting type corrosion behavior was seen for both untreated and all treated samples. The corrosion behaviors changed depending on the nitriding temperature. It was observed from polarization graphs that corrosion potential values decreased as treatment temperatures increased. The untreated sample showed pitting corrosion behavior in 1.2×10^{-6} A·cm^{-2} current density and -4×10^{-1} V potential values. On the other hand, it was examined that the corrosion behaviors of the nitrided samples were affected by chemical composition and thickness of the modified layers. Treatment temperature led to changes in the phase and the thickness of the modified layer. If modified layer is thick enough and is not composed of nitride phases, corrosion resistance of 316L stainless steel does not change after nitriding. These conditions were obtained from the samples nitrided at 350 ˚C. As seen in Fig. 6, current density-potential curve of untreated sample is similar to that of the nitrided sample at 350 ˚C. At this treatment temperature, modified layer was very thin and this layer consisted of mostly s-phase. Similar studies supported that if modified layer included s-phases corrosion resistance could be higher than untreated samples. Fossati *et al*.[21] reported that the corrosion properties of s-phase depended on the high nitrogen concentration in the structure. It was also remarked that pitting corrosion resistance improved even though slightly amount of interstitial nitrogen atoms existed in austenitic stainless steels[26]. When modified layer containing the s-phase is subjected to corrosion, the nitrogen atoms that are interstitial atoms, release from structure, and these atoms react with H^+ ions thus, NH_4 occurs[21]. It was thought that NH_4 formation decreased the electron less from metal substrate and caused passivation. During nitriding above 400 ˚C, occurring CrN in modified layer caused to the inadequate passivation and the increasing corrosion rate because the amount of free Cr atoms decreased in the structure. Consequently, pitting corrosion was seen from the corroded surfaces. The SEM images in Fig. 7

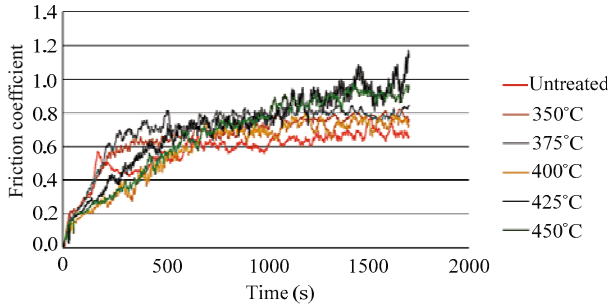

Fig. 5 Friction coefficient versus time behavior of untreated and plasma nitrided samples.

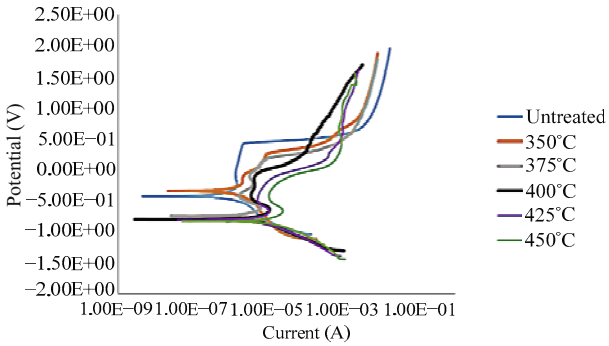

Fig. 6 Current density-potential curves of untreated and treated samples.

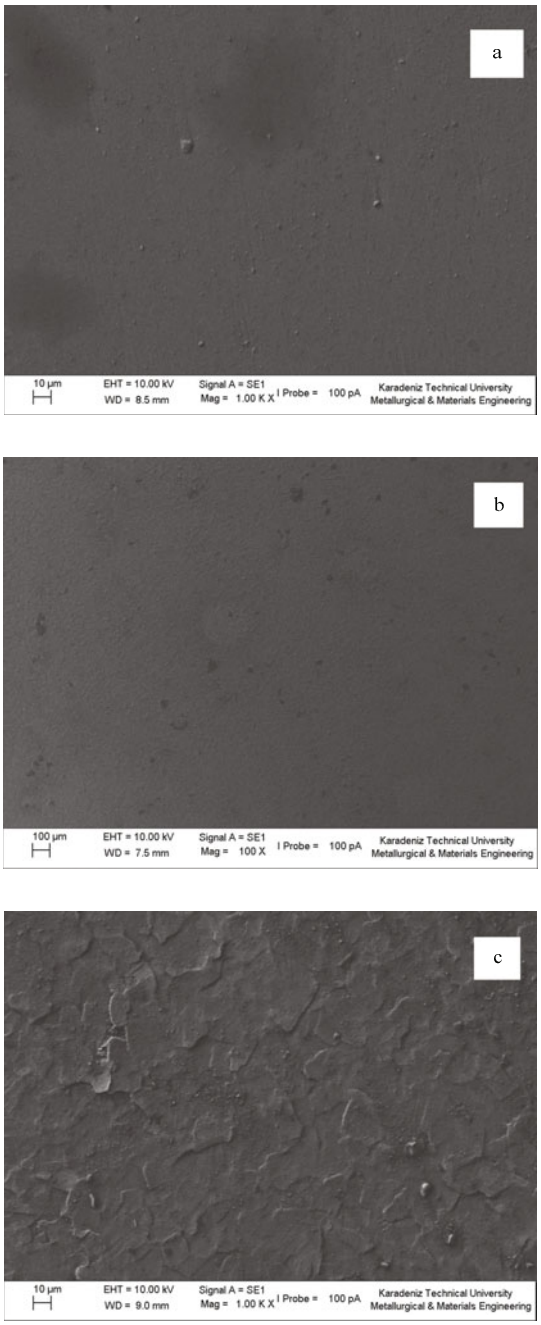

Fig. 7 SEM micrograph of the samples exposed to corrosion tests (a) 350 ˚C; (b) 400 ˚C; (c) 450 ˚C.

indicated that the pitting corrosion was effective corrosion mechanism for all the specimens.

The surfaces of the samples nitrided at temperatures lower than 400 ˚C were almost undamaged. When the XRD graphs and SEM images are evaluated together, it can be said that if the surface of the nitrided 316L stainless steel is resistant to the corrosion, the modified layer has to be thick enough and this layer should be mainly consisted of the s-phase. At the temperatures higher than 400 ˚C, CrN+ γ'-Fe_4N dual phase structure begins to form in the modified layer and it behaves like a galvanic cell because of potential difference between CrN and γ'-Fe_4N phases[21]. In this case, the corrosion resistance of the 316Lstainless steel samples decreases. Therefore, while the surfaces of samples nitrided at temperatures lower than 400 ˚C were almost undamaged (Figs. 7 a and 7b), and it was observed that many pits appeared on the surface of nitrided samples at temperatures higher than 400 ˚C (Fig 7c).

3.6 Magnetic measurements

Fig. 8 shows the VSM results of the untreated and treated 316L samples. According to the VSM analysis, ferromagnetism in the modified layer is revealed by the observation of the hysteresis loops. A considerable change in magnetic moment was seen in Fig. 8 and it was attributed to the treatment temperature. The hysteresis loops of samples reduced with the increase in nitriding temperature. While the lowest hysteresis loop area was seen from the sample nitrided at 450˚C, the highest hysteresis loop area was obtained from the untreated sample. The nitrided samples tend to be ideal ferromagnetic behavior with the increase in nitriding temperature. That is, the substance is not magnetized, after the external field is removed[27]. The XRD analysis indicated that the fcc structure of treated 316L stainless steel didn't change until 450 ˚C and the nitrogen atoms didn't bond with the Fe atoms in nitrided specimens[1,6]. The magnetization is one of the most important parameters affecting the interatomic distance. Plasma nitriding is a diffusion process and the activation of nitrogen atoms increases with nitriding temperature. After diffusion, nitrogen atoms trapped inside interatomic. Austenite lattice expands due to the effect of nitrogen atoms[19,28]. Consequently, nitrogen leads to lattice expansion and magnetic interactions are influenced because of the increase in Fe-Fe distance[29,30]. This study suggested that the lattice expansion is related to both changing temperature and thickness of the modified layer.

3.7 Electrical properties

The electrical resistivity of the untreated and treated samples is shown in Fig. 9. It was observed that the resistivity value of untreated samples was lower than those of nitrided samples. Moreover, the resistivity

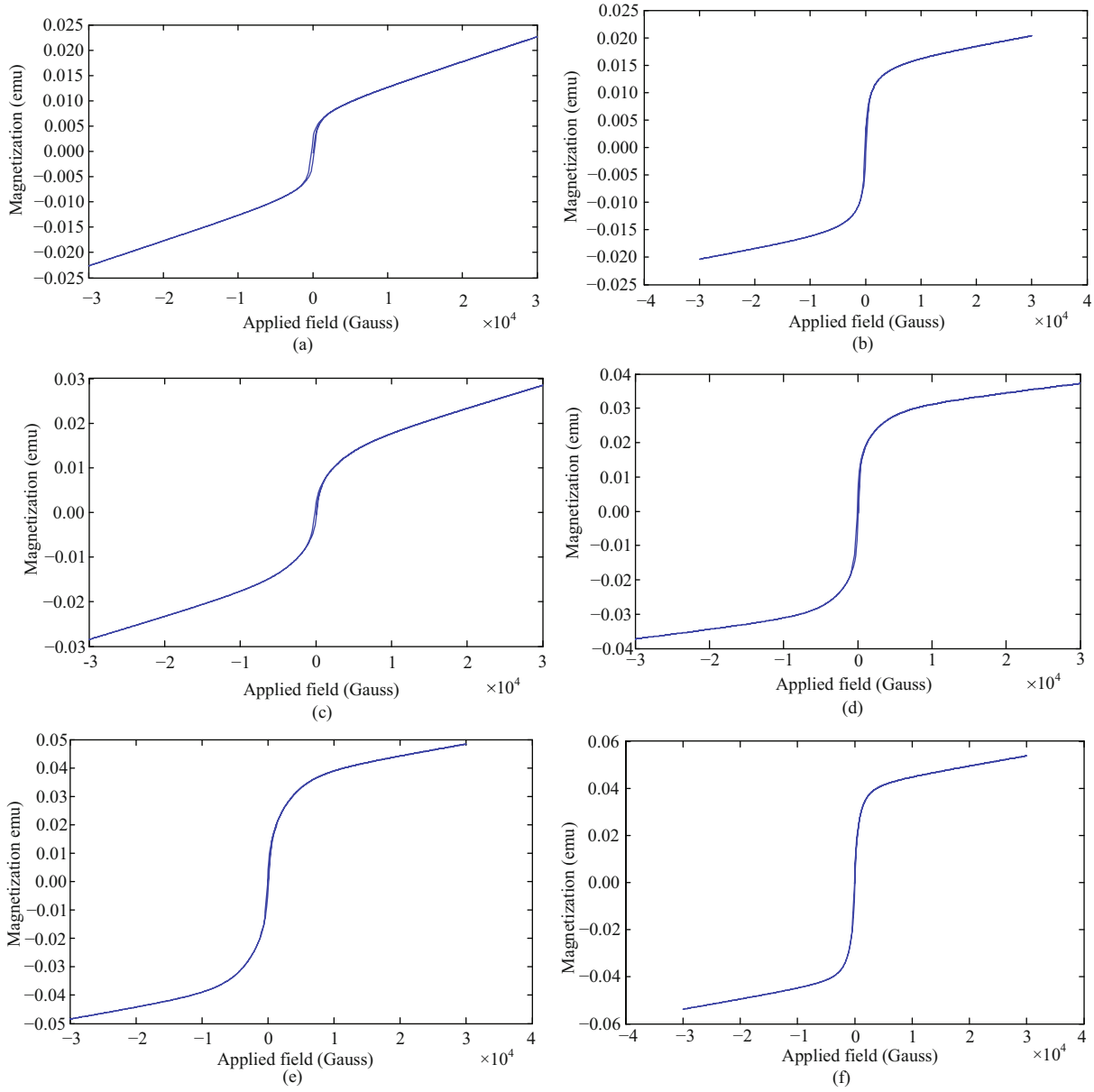

Fig. 8 VSM measurements for the untreated and treated 316L samples. (a) Untreated; (b) 350 ˚C; (c) 375 ˚C; (d) 400 ˚C; (e) 425 ˚C and (f) 450 ˚C.

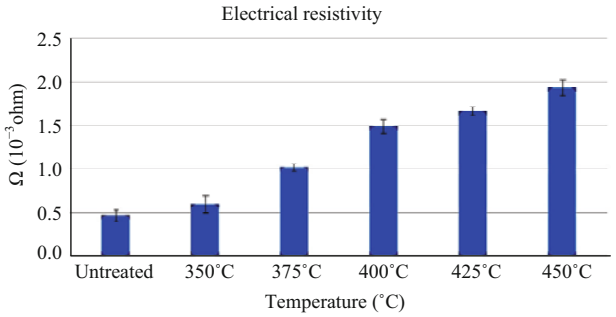

Fig. 9 The electrical resistivity of untreated and treated samples.

values increased with nitriding temperature. The highest value was obtained from the sample nitrided at 450 ˚C. It can be seen from Fig. 1 that CrN phase occurred in the modify layer at the higher nitriding temperatures. This structure is in ceramic form and it has dielectric property[31]. This dielectric structure may cause electrical resistivity. When the treatment temperature reached 450 ˚C, the amount of the CrN increased, thus electrical resistivity increased.

4 Conclusion

In this study, 316L stainless steel samples were plasma nitrided at different temperatures and the properties of the untreated and plasma nitrided samples were

experimentally investigated. After plasma nitriding, the modified layer was obtained on the 316L stainless steel surface. In the modified layer mainly s-phases, CrN and γ'-Fe_4N structures were formed depending on treatment temperature. While the s-phase mainly occurred at the nitriding temperatures lower than 400 ˚C, the CrN and γ'-Fe_4N phases formed at the temperatures above 400 ˚C. The morphology, roughness, hardness and thickness of the modify layers strongly depended on treatment temperature. The surface roughness, hardness and thickness increased with the treatment temperature. The wear resistance of 316L stainless steel improved significantly with plasma nitriding, which increased with treatment temperature. The corrosion behaviors of the nitrided specimens were related to the thickness of continuous modified layer and phase type that occurred during nitriding. The electrical resistivity and the soft (ideal) ferromagnetic of 316L stainless steel increased with treatment temperature during nitriding treatment. The ferromagnetic behavior of the s-phase was close to the ideal ferromagnetic material behavior like untreated 316L stainless steel. It can be overall summarized that if the modified layer consisting of mainly s-phase formed on the surface, plasma nitriding can be applied to 316L stainless steel as biomedical material from the point of wear, corrosion, magnetic and electrical properties.

Acknowledgment

Authors would like to thank the officials of The ETU Central Laboratory for their precious contribution.

References

[1] Nosei L, Avalos M, Gómez B, Nachez L, Feugeas J. Stability under temperature of expanded austenite developed on stainless steel AISI 316L by ion nitriding. *Thin Solid Films*, 2004, **468**, 134–141.

[2] Wang J, Xiong J, Peng Q, Fan H, Wang Y, Li G, Shen B. Effect of DC plasma nitriding parameters on microstructure and properties of 304L stainless steel. *Materials Characterization*, 2009, **60**, 197–203.

[3] Wang Q, Zhang L, Dong J. Effects of plasma nitriding on microstructure and tribological properties of CoCrMo alloy implant materials. *Journal of Bionic Engineering*, 2010, **7**, 337–344.

[4] Yetim A F, Alsaran A, Çelik A. Investigation of tribological and electrochemical properties of dual layer after low temperature plasma carbo-nitriding. *Surface Engineering*, 2010, **26**, 178–184.

[5] Yetim A F, Alsaran A, Çelik A, Efeoglu I. Corrosion behaviour of Ti-DLC deposition on prenitrided 316L stainless steel and Ti-6Al-4V alloy. *Corrosion Engineering Science and Technology*, 2011, **46**, 439–444.

[6] Yıldız F, Yetim A, Alsaran A, Çelik A, Kaymaz İ. Fretting fatigue properties of plasma nitrided AISI 316L stainless steel: Experiments and finite element analysis. *Tribology International*, 2011, **44**, 1979–1986.

[7] Puchi-Cabrera E, Staia M, Ochoa-Pérez E, Teer D, Santana-Méndez Y, La Barbera-Sosa J, Chicot D, Lesage J. Fatigue behavior of a 316L stainless steel coated with a DLC film deposited by PVD magnetron sputter ion plating. *Materials Science and Engineering*: *A*, 2010, **527**, 498–508.

[8] Arslan E, İğdil M C, Trabzon L, Kazmanlı K, Gulmez T. The corrosion behaviour of austenitic 316L stainless steel after low-T plasma nitridation in the physiological solutions. *Plasma Processes and Polymers*, 2007, **4**, S717–S720.

[9] Luo Y, Yang L, Tian M. Influence of bio-lubricants on the tribological properties of Ti6Al4V alloy. *Journal of Bionic Engineering*, 2013, **10**, 84–89.

[10] Nosei L, Farina S, Ávalos M, Náchez L, Gómez B, Feugeas J. Corrosion behavior of ion nitrided AISI 316L stainless steel. *Thin Solid Films*, 2008, **516**, 1044–1050.

[11] Menthe E, Bulak A, Olfe J, Zimmermann A, Rie K-T. Improvement of the mechanical properties of austenitic stainless steel after plasma nitriding. *Surface and Coatings Technology*, 2000, **133-134**, 259–263.

[12] Ichii K, Fujimura K, Takase T. Structure of the ion-nitrided layer of 18-8 stainless steel. *Technical Report of Kansai University*, 1986, 135–144.

[13] Singh V, Marchev K, Cooper C, Meletis E. Intensified plasma-assisted nitriding of AISI 316L stainless steel. *Surface and Coatings Technology*, 2002, **160**, 249–258.

[14] Gontijo L C, Machado R, Casteletti L C, Kuri S E, Nascente P A P. Study of the s phases formed on plasma-nitrided austenitic and ferritic stainless steels. In Chandra T, Wanderka N, Reimers W, Ionescu M (eds.), *Thermec* 2009, Trans Tech Publications Ltd, Stafa-Zurich, Switzerland, 2010, 775–780.

[15] Williamson D L, Davis J A, Wilbur P J, Vajo J J, Wei R, Matossian J N. Relative roles of ion energy, ion flux, and sample temperature in low-energy nitrogen ion implantation of Fe-Cr-Ni stainless steel. *Nuclear Instruments and Methods in Physics Research Section B: Beam Interactions with Materials and Atoms*, 1997, **127**, 930–934.

[16] Blawert C, Mordike B, Jirásková Y, Schneeweiss O. Structure and composition of expanded austenite produced

by nitrogen plasma immersion ion implantation of stainless steels X6CrNiTi1810 and X2CrNiMoN2253. *Surface and Coatings Technology*, 1999, **116**, 189–198.

[17] Omari M A, Sevostianov I. Evaluation of the growth of dislocations density in fatigue loading process via electrical resistivity measurements. *International Journal of Fracture*, 2013, **179**, 229–235.

[18] Kokubo T, Takadama H. How useful is SBF in predicting in vivo bone bioactivity? *Biomaterials*, 2006, **27**, 2907–2915.

[19] Yetim A F, Yildiz F, Alsaran A, Çelik A. Surface modification of 316L stainless steel with plasma nitriding. *Kovove Materialy-Metallic Materials*, 2008, **46**, 105–116.

[20] Rohde U L, Poddar A K, Patel P, Badea D, Schoepf K J. *Low Thermal Drift*, *Tunable Frequency Voltage Controlled Oscillator*, Google Patents, No:US7262670 B2–2007.

[21] Fossati A, Borgioli F, Galvanetto E, Bacci T. Glow-discharge nitriding of AISI 316L austenitic stainless steel: Influence of treatment time. *Surface and Coatings Technology*, 2006, **200**, 3511–3517.

[22] Sun Y, Li X, Bell T. X-ray diffraction characterisation of low temperature plasma nitrided austenitic stainless steels. *Journal of Materials Science*, 1999, **34**, 4793–4802.

[23] Borgioli F, Fossati A, Galvanetto E, Bacci T, Pradelli G. Glow discharge nitriding of AISI 316L austenitic stainless steel: Influence of treatment pressure. *Surface and Coatings Technology*, 2006, **200**, 5505–5513.

[24] Smith A. The friction and sliding wear of unlubricated 316 stainless steel at room temperature in air. *Wear*, 1984, **96**, 301–318.

[25] Sun Y, Bell T. Silinding wear characteristics of low temperarure plasma nitrided 316 austenitic stainless steel. *Wear*, 1998, **218**, 34–42.

[26] Borgioli F, Fossati A, Galvanetto E, Bacci T. Glow-discharge nitriding of AISI 316L austenitic stainless steel: influence of treatment temperature. *Surface and Coatings Technology*, 2005, **200**, 2474–80.

[27] Wei B, Shima M, Pati R, Nayak S K, Singh D J, Ma R,Li Y, Bando Y, Nasu S, Ajayan P M. Room-temperature ferromagnetism in doped face-centered cubic Fe nanoparticles. *Small*, 2006, **2**, 804–809.

[28] Hannula S-P, Nenonen P, Hirvonen J-P. Surface structure and properties of ion-nitrided austenitic stainless steels. *Thin Solid Films*, 1989, **181**, 343–350.

[29] Öztürk O, Okur S, Riviere J. Structural and magnetic characterization of plasma ion nitrided layer on 316L stainless steel alloy. *Nuclear Instruments and Methods in Physics Research Section B: Beam Interactions with Materials and Atoms*, 2009, **267**, 1540–1545.

[30] Akamatsu K. Stainless steel 2000. *Proceedings of an International Current Status Seminar on Thermochemical Surface Engineering of Stainless Steel*, *Maney Publ.*, *London*, 2000.

[31] Abedi H, Salehi M, Yazdkhasti M, Hemmasian-E A. Effect of high temperature post-oxidizing on tribological and corrosion behavior of plasma nitrided AISI 316 austenitic stainless steel. *Vacuum*, 2010, **85**, 443–447.